

Nonlinearity in the Dynamics of Photoinduced Nucleation Process

Kunio Ishida*

Corporate Research and Development Center, Toshiba Corporation, 1 Komukaitoshiba-cho, Saiwai-ku, Kawasaki 212-8582, Japan

Keiichiro Nasu

Solid State Theory Division, Institute of Materials Structure Science, KEK, Graduate University for Advanced Study, and CREST JST, 1-1 Oho, Tsukuba, Ibaraki 305-0801, Japan

(Received 21 August 2007; published 20 March 2008)

Coherent nonlinear dynamics of photoinduced cooperative phenomena at 0 K is studied by numerical calculations on a model of molecular crystals. We found that the photoinduced nucleation process is triggered only when a certain amount of excitation energy is supplied in a narrow part of the system; i.e., there exists the smallest size of the cluster of excited molecules which makes the nucleation possible. As a result, the portion of the cooperatively converted molecules is nonlinearly dependent on the photoexcitation strength, which has been observed in various materials.

DOI: [10.1103/PhysRevLett.100.116403](https://doi.org/10.1103/PhysRevLett.100.116403)

PACS numbers: 71.35.Lk, 05.45.-a, 64.70.Nd, 78.20.Bh

The discovery of photoinduced cooperative phenomena has attracted our attention to new aspects of nonequilibrium dynamics of excited states in condensed matter [1–13]. It has been pointed out that two important situations should be considered to understand the mechanism of photoinduced cooperativity. In the first one, photoexcited electrons are itinerant and long-range interaction between atoms is induced by them. As a result macroscopic structural change takes place following the appearance of lattice instability [8]. The second one, which we focus on in this Letter, concerns the excitation of localized electrons in each molecular unit followed by the nucleation process due to intermolecular interactions. In this case the nucleation process is driven by the energy transfer process between molecular units through excitation of vibrational modes (phonons), and the dynamical properties of the atomic motion and the electronic states are particularly important. We also note that, in the very initial stages of the nucleation process, the coherent nature of the quantum-mechanical states of electrons and phonons plays a dominant role, and that the nonadiabaticity of the electrons and phonons should be taken into account to pursue the dynamics of the system.

We have proposed a model of molecular crystals which describes the coherent dynamics of the initial nucleation process of photoinduced domain growth at 0 K. Calculating the numerical solutions of the time-dependent Schrödinger equation, we found that initially excited molecules become a trigger to domain growth, and that they show various spatial patterns in coherent regime [11–13]. In this Letter, we study photoinduced nucleation processes focusing on the case in which multiple photons are absorbed and many domains are generated simultaneously. In this case the dynamics of the excited states is reduced to a pattern formation problem of excited molecules, and our aim is to discuss the nonlinearity between excited energy distribution and pattern formation dynamics in the coherent regime.

Nonlinear dynamics of spatiotemporal pattern formation has been extensively studied to understand the various aspects of nonequilibrium phenomena in wide scale-range, e.g., from nanoscale of the Belousov-Zhabotinsky reaction or the phase separation dynamics in the kinetic Ising model [14,15] to the astronomical scale of cosmic structure formation [16]. It has been pointed out that the density fluctuation of relevant physical properties becomes “seeds” of growing patterns, and that the initial density distribution determines their geometrical structure. Thus, in analogy to these cases, we obtain an idea to study the coherent dynamics of photoinduced nucleation process in the presence of excitation density fluctuation. However, the above results of stochastic simulations basically describe the kinetics of the system, and do not correspond to the dynamics of the wave functions in the coherent regime; i.e., the nonadiabaticity of electrons and phonons cannot be taken into account by stochastic simulations. Although the effect of decoherence eliminates such coherent properties within a few picosecond after photoexcitation, the very first process of photoinduced cooperativity should be discussed in an ideal situation, i.e., in a coherent regime. Therefore, we require a theoretical study of coherent pattern formation based on the deterministic solution of the time-dependent Schrödinger equation in order to clarify and understand the nonlinear nature of the photoinduced cooperativity.

To describe the present model, we first point out that one of the elementary processes of the photoinduced nucleation in this system is the nonadiabatic transition between the ground and the excited electronic states in each molecule. Electrons relevant to this process are assumed to be localized in each molecule, and two electronic levels corresponding to the ground and excited electronic states are taken into account per molecule. In each of the molecules we assume the diabatic potential energy surfaces with a single relevant vibration mode which cross each other, and the nonadiabaticity in the dynamics is taken into account via “spin-flip” interaction between two electronic states as

in the studies of the nonadiabatic transitions in typical organic molecules [17]. As for the intermolecular interaction, we take into account the bilinear coupling terms between distortion of adjacent molecules and the dipole-dipole interaction between excited-state electrons of which the strength varies with the molecular distortion. Furthermore, the interaction which describes the molecular distortion induced by the excited-state electrons in the adjacent molecules is also considered. Hence, the Hamiltonian in the present study is described as follows:

$$\begin{aligned} \mathcal{H} = & \sum_{\vec{r}} \left\{ \frac{p_{\vec{r}}^2}{2} + \frac{\omega^2 u_{\vec{r}}^2}{2} \right. \\ & + (\sqrt{2\hbar\omega^3} s u_{\vec{r}} + \varepsilon \hbar \omega + s^2 \hbar \omega) \hat{n}_{\vec{r}} + \lambda \sigma_x^{\vec{r}} \left. \right\} \\ & + \sum_{\langle \vec{r}, \vec{r}' \rangle} [\alpha \omega^2 (u_{\vec{r}} - \beta \hat{n}_{\vec{r}})(u_{\vec{r}'} - \beta \hat{n}_{\vec{r}'}) \\ & - \{V - W(u_{\vec{r}} + u_{\vec{r}'})\} \hat{n}_{\vec{r}} \hat{n}_{\vec{r}'}], \end{aligned} \quad (1)$$

where $p_{\vec{r}}$ and $u_{\vec{r}}$ are the momentum and coordinate operators for the vibration mode of a molecule at site \vec{r} , respectively. The electronic states at site \vec{r} are denoted by $|\downarrow\rangle_{\vec{r}}$ (ground state) and $|\uparrow\rangle_{\vec{r}}$ (excited state) and $\sigma_i^{\vec{r}}$ ($i = x, y, z$) are the Pauli matrices which act only on the electronic states of the molecule at site \vec{r} . $\hat{n}_{\vec{r}}$ denotes the density of the electron in $|\uparrow\rangle_{\vec{r}}$ which is rewritten as $\hat{n}_{\vec{r}} = \sigma_z^{\vec{r}} + 1/2$. The second sum which gives the intermolecular interaction is taken over all the pairs on nearest neighbor sites, and the vibrational period of an individual molecule is denoted by $T = 2\pi/\omega$. The vibration modes are quantized in order to describe the nonadiabatic transition between potential energy surfaces rigorously. We note that this Ising-like model is similar to the one to study the thermodynamical properties of the Jahn-Teller effect [18], though the nonequilibrium dynamics of the excited states in the model has not been understood.

We chose the values of the parameters as $\varepsilon = 2.3$, $s = 1.4$, $V = 1.1$, $W = 0.2$, $\alpha = 0.1$, $\beta = 0.2$, and $\lambda = 0.2$. Although those values are typical for organic molecules as for electron-vibration coupling [19] and the intermolecular Coulomb interaction, we mention that the other parameters are not easy to determine their values either from theoretical calculations or experimental results.

The numerical solutions of the time-dependent Schrödinger equation for the Hamiltonian (1) were obtained by the Runge-Kutta method with various initial conditions. In each series of simulations, the dynamics of the system on a 96×96 lattice with periodic boundary conditions was calculated. We also applied a mean-field approximation in which the contribution of the wave function at the nearest neighbor sites is substituted by the average value with respect to the wave function $|\Phi(t)\rangle$, which is also quite suitable for large scale computing with a grid environment, for example. The details of the model and the calculation method are described in Ref. [12].

We have pointed out that the population of the excited electronic state $\tilde{N}(\vec{r}, t) = \langle \Phi(t) | \hat{n}_{\vec{r}} | \Phi(t) \rangle$ is suitable to discuss the dynamics of the spatial patterns of the photo-induced domains. In particular, the sum of the excited-state population $N(t) = \sum_{\vec{r}} \tilde{N}(\vec{r}, t)$ gives a measure to estimate the size of the photoinduced domain [12], which is shown in Fig. 1 as functions of time for several initial conditions. The dotted line in Fig. 1 shows that an isolated excited molecule does not trigger the nucleation processes but loses the excitation energy after a few periods of the molecular vibration mode. When two excited molecules are placed on the nearest neighbor sites, the potential energy barrier between $|\downarrow\rangle_{\vec{r}}$ and $|\uparrow\rangle_{\vec{r}}$ in these molecules is still too high to make the electronic state conversion possible. Thus no domain growth occurs, though these molecules do not go back to the ground state within the simulation time (see the dot-dashed line in Fig. 1). On the contrary, when the initially excited molecules form an *I*-tromino or an *I*-tetromino, $N(t)$ increases as the excitation energy is transferred to the other molecules, and a photoinduced domain grows as shown in the solid line and the dashed line in Fig. 1.

The above results clearly show that there exists a smallest cluster of excited molecules which leads to the domain growth after photoexcitation; i.e., a certain amount of excitation energy is required to be initially concentrated in a narrow spatial area of the system. The dynamics of the photoexcited states differs qualitatively from each other as the initial state is varied, and, in particular, the size of the domain is not simply determined by the value of $N(0)$. To be more precise, the domain growth dynamics reflects the symmetry of the initial configuration as well as the concentration of excitation energy. A taxonomic study of the

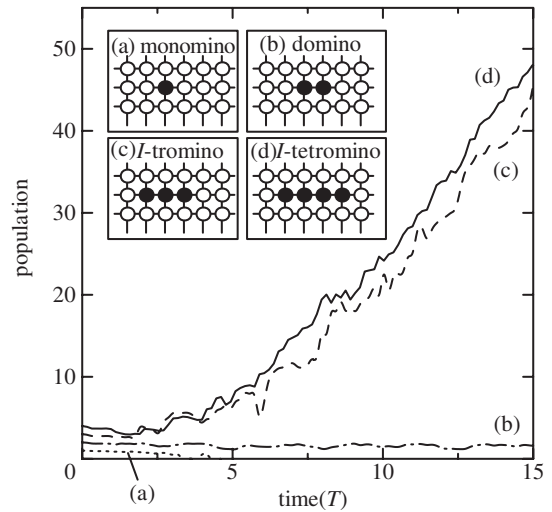


FIG. 1. Population of the excited-state molecule $N(t)$ as functions of time. Inset: initial configurations of excited molecules. the filled circles and the open circles correspond to the molecules in the Franck-Condon state and the ground state, respectively.

domain growth dynamics with respect to the configuration of initial excited molecules will be given elsewhere.

Although the size of the smallest cluster for the domain growth depends on the values of the parameters, we also stress that our simple model which consists only of localized electrons and molecular vibration modes is sufficient to discuss the nonlinearity of the nucleation process.

We extended our calculations to the cases where initially excited molecules are distributed at random, and studied the pattern formation dynamics of excited-state domains during the initial nucleation processes in coherent regime. In this case, the excitation ratio ρ , defined by the ratio of the number of the initially excited molecules to the total number of the molecules, is a relevant parameter. Figure 2 shows the gradation maps of $\tilde{N}(\vec{r}, t)$ for $t = 0$, $t = 7.5T$, and $t = 15T$ for $\rho = 0.0625$. At $t = 0$ the distribution of the excited molecules is not uniform, and thus the fluctuation of $\tilde{N}(\vec{r}, t)$ is present. When excited molecules are densely concentrated in certain parts of the system, the molecules around them are able to overcome the potential energy barrier to make the electronic state conversion, and thus the excited-state domain starts to grow there. On the contrary, when the density of the excited molecules is not sufficiently high for the domain growth, the excitation energy is released to the other molecules through the vibrational coupling α , and thus the excited molecules return to the ground state. As a result, we obtain islands of photoinduced domains shown in Fig. 2(b) around the parts of the system which are initially supplied with higher excitation energy. Each island has a fine structure corresponding to its multifractal properties [13], and the islands merge with each other to make larger ones as shown in Fig. 2(c), and $N(t)$ continues to increase with time. Thus, the density fluctuation of the initially excited molecules reflects the structure of the photoinduced domains, and vice versa. These results directly reflect the discussion on the smallest cluster for the domain growth shown previously. We also note that, observing the domain growth process shown in Figs. 2(a) and 2(c), we also found that the finite-size effect will not be negligible in the present case, when the system size is comparable to the size of the islands of the excited molecules.

We also found that the size of the photoinduced domains nonlinearly depends on the excitation ratio ρ . Figure 3 shows the conversion ratio c_ρ defined by $c_\rho = N(t = 15T)/M$ as a function of ρ , where M is the number of molecules and is $9216 (= 96^2)$ in the present calculations. To obtain these results we calculated the average value of c_ρ for each value of ρ over 64 series of simulations as in the calculation of R .

Figure 3 shows that c_ρ depends on ρ as $\sim \rho^3$ in the dilute limit ($\rho \sim 0$), and deviates from ρ^3 for $\rho > 0.1$. This feature reflects the size of the smallest cluster which enables domain growth. With a fixed value of ρ , the smallest clusters for domain growth (a tromino) appear in the initial

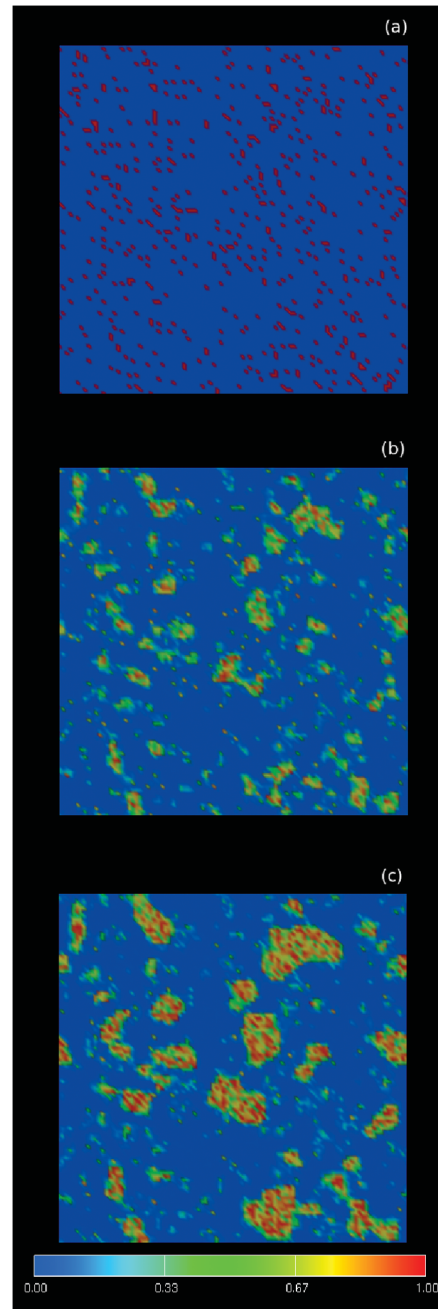


FIG. 2 (color). Gradation maps of excited-state population $\tilde{N}(\vec{r}, t)$ on a 96×96 lattice for $\rho = 0.0625$ for (a) $t = 0$, (b) $t = 7.5T$, and (c) $t = 15T$.

state with a probability proportional to ρ^3 in the dilute limit. Hence, only a portion of the initially excited molecules contributes to the domain growth. As we can neglect the interference between domains for $\rho \sim 0$, the number of converted molecules is proportional to ρ^3 in this case.

As ρ increases, the growing domains interfere with each other and the growth rate becomes lower. Thus c_ρ deviates from ρ^3 as the value of ρ increases as shown in Fig. 3. In any case, the conversion ratio increases as ρ^m where m is

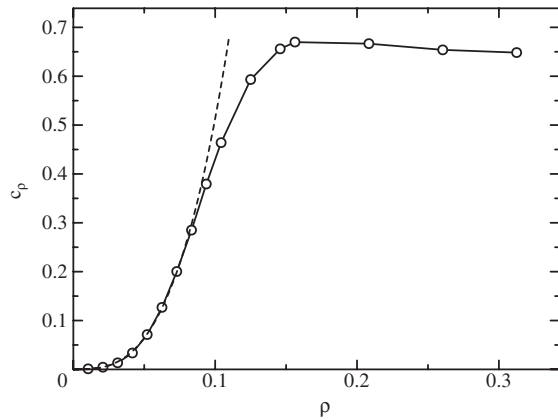


FIG. 3. Conversion ratio c_ρ as a function of excitation ratio ρ . The dashed line which is proportional to ρ^3 is drawn as a guide for the eyes.

the size of the smallest cluster which triggers the nucleation processes. If m is experimentally determined through the measurement of optical properties, for example, we will have a clue to understand the microscopic mechanism of the elementary process of the domain growth dynamics.

Figure 3 also shows that $c_\rho/\rho < 7$ in the present case, although some larger values were reported in experimental studies [2–5]. Larger values of c_ρ/ρ were found in materials close to their critical temperature, since instability of thermodynamical state of the system enhances the conversion ratio. We mention that, as the temperature is raised and approaches to the critical temperature for the structural phase transition, the value of c_ρ/ρ will increase. Furthermore, we should note that the present calculations are valid before the decoherence of vibrational states takes place, and that the value of c_ρ shown in Fig. 3 corresponds to that for $t \sim 3$ psec for $T \sim 200$ fsec as in typical organic molecules. We, however, expect that the domains continue to grow after the decoherence occurs, and thus the experimentally obtained conversion ratio cannot be directly compared with the present results quantitatively. We stress that the nonlinearity of conversion ratio as a function of ρ is essentially understood by the initial process of the domain growth, and that the present calculations are of importance in order to understand the microscopic mechanism of the photoinduced cooperativity.

Summarizing the present Letter, we conclude that the coherent nonlinear dynamics of the photoinduced domain growth at 0 K is understood by a model of localized electrons coupled with molecular vibration mode shown by Eq. (1). We found that there exists a smallest cluster of excited molecules which is required to induce the domain growth, and that the initial nucleation process does not start unless sufficient energy is concentrated in a narrow area of

the system. When the fluctuation of excitation density realizes the formation of such clusters, photoinduced nucleation is triggered to form domains afterwards, and thus the excitation energy fluctuation determines the domain structure. We also showed that the nonlinearity of the conversion ratio as a function of excitation ratio is understood as a result of the interdomain interactions besides the above effect.

Lastly we mention that the present results will give a perspective to the future experimental studies on the coherent dynamics of photoinduced structure change by time-resolved x-ray diffraction measurement. Since strong coherent x-ray sources are under development [20], it will be possible to observe the dynamics of the nucleation process and pattern formation process in coherent regime with femtosecond resolution, and the present results will be compared with them to understand the physics of photoinduced cooperativity.

K. I. is grateful to K. Takaoka, H. Asai, and S. Nunoue for helpful advice. This work was supported by the Next Generation Super Computing Project, Nanoscience Program, MEXT, Japan, and the numerical calculations were carried out on the computers at the Research Center for Computational Science, National Institutes of Natural Sciences.

*ishida@arl.rdc.toshiba.co.jp

- [1] *Photoinduced Phase Transitions*, edited by K. Nasu (World Scientific, Singapore, 2004).
- [2] S. Koshihara *et al.*, *J. Phys. Chem. B* **103**, 2592 (1999).
- [3] S. Koshihara *et al.*, *Phys. Rev. B* **52**, 6265 (1995).
- [4] S. Iwai *et al.*, *Phys. Rev. Lett.* **88**, 057402 (2002).
- [5] A. Mino *et al.*, *Mol. Cryst. Liq. Cryst.* **314**, 107 (1998).
- [6] N. O. Moussa *et al.*, *Phys. Rev. Lett.* **94**, 107205 (2005).
- [7] J. S. Costa *et al.*, *J. Phys. Conf. Ser.* **21**, 67 (2005).
- [8] D. M. Fritz *et al.*, *Science* **315**, 633 (2007).
- [9] K. Koshino and T. Ogawa, *Phys. Rev. B* **58**, 14 804 (1998).
- [10] H. Mizouchi and K. Nasu, *J. Phys. Soc. Jpn.* **69**, 1543 (2000).
- [11] K. Ishida, *Phys. Status Solidi C* **3**, 3438 (2006).
- [12] K. Ishida and K. Nasu, *Phys. Rev. B* **76**, 014302 (2007).
- [13] K. Ishida and K. Nasu, *J. Phys. Condens. Matter* **20**, 025212 (2008).
- [14] S. van Gemmert *et al.*, *Phys. Rev. E* **72**, 046131 (2005).
- [15] P. C. Hohenberg and B. I. Halperin, *Rev. Mod. Phys.* **49**, 435 (1977).
- [16] V. Springel *et al.*, *Nature (London)* **435**, 629 (2005).
- [17] L. Salem, *Science* **191**, 822 (1976).
- [18] K. Boukheddaden, *Prog. Theor. Phys.* **112**, 205 (2004).
- [19] K. Ishida *et al.*, *J. Chem. Phys.* **127**, 194304 (2007); K. Horikoshi *et al.*, *J. Chem. Phys.* **127**, 054104 (2007).
- [20] T. Shintake *et al.*, *Proc. SPIE-Int. Soc. Opt. Eng.* **4500**, 12 (2001).